Available online at www.sciencedirect.com

ScienceDirect

ELSEVIER

Journal of Nuclear Materials 367–370 (2007) 1150–1154

journal of nuclear materials

www.elsevier.com/locate/jnucmat

Investigation of Pb–Li compatibility issues for the dual coolant blanket concept

B.A. Pint [*], J.L. Moser, P.F. Tortorelli

Metals and Ceramics Division, Oak Ridge National Laboratory, Oak Ridge, TN 37831-6156, United States

---

Abstract

One proposed blanket concept uses advanced ferritic alloys and a SiC/SiC composite flow channel insert with both Pb–17 at.%Li and He coolants. As the first step in determining the long-term compatibility of SiC/SiC in Pb–Li, specimens of high-purity, chemical vapor deposited (CVD) SiC were exposed in capsules for up to 5000 h at 800 °C and 1000 h at 1200 °C. Dissolved Si was detected in the Pb–Li after the highest temperature exposures suggesting that SiC may be limited to <1100 °C in Pb–Li. Aluminide coatings are being considered for corrosion resistant coatings for the tubing between the first wall and the heat exchanger. Initial results indicate that, in Pb–Li at 700 °C, FeCrAl, Fe_3Al and NiAl form a protective alumina layer which reduces dissolution compared to type 316 stainless steel.

---

1. Introduction

Among the proposed fusion blanket concepts, one possibility is a dual coolant (He and Pb–Li) system using advanced ferritic steels as the structural material and a silicon carbide composite as a flow channel insert [1,2]. Although the ITER test blanket module (TBM) design will operate at <500 °C, thereby limiting compatibility problems, ultimately this concept would be more attractive with a maximum operating temperature of 700–800 °C. In this temperature range, critical compatibility issues need to be addressed. Recent effort has been focused on the compatibility of ferritic–martensitic steels in Pb–Li at 400–600 °C [3,4]. However, there has been less work examining SiC/SiC composites and corrosion-resistant coatings needed at higher temperatures.

The compatibility of SiC/SiC composites with Pb–17Li is of interest, both as a non-structural, flow channel insert to reduce corrosion and the MHD pressure drop, and as a higher temperature (1000–1100 °C) structural material [5]. SiC dissolves readily in Li at <500 °C [6]. However, the activity of Li is much lower in Pb–17Li (e.g., 1.2×10^{-4} at 500 °C) [7] such that the native surface oxide on SiC, SiO_2, is stable. The same argument applies for Al-containing alloys or coatings that could form a protective external Al_2O_3 in Pb–Li [8]. Coatings are of interest for tubing materials to carry Pb–Li from the first wall to the heat exchanger at ~700 °C. While a SiC flow channel insert could protect the steel walls from Pb–Li dissolution, it is

---

[*] Corresponding author. Tel.: +1 865 576 2897; fax: +1 865 241 0215.

E-mail address: pintba@ornl.gov (B.A. Pint).

0022-3115/$ - see front matter Published by Elsevier B.V.
doi:10.1016/j.jnucmat.2007.03.206

unlikely this strategy could be used through the entire flow path. Because of the complex geometry, a durable, defect-free coating is needed but not easily achieved. Contact of Fe- or Ni-base, alloys with flowing Pb–Li at ~700 °C would result in unacceptably high dissolution rates [3,4,9]. Although the use of refractory metals is one option, [10] fabrication and durability of Nb or Mo tubing could be an issue. A protective coating could allow a conventional Fe- or Ni-base tubing alloy to be used.

Baseline compatibility data is being developed using static capsule tests and model materials. Studying monolithic SiC avoids issues with composites, such as fiber interfaces and porosity. Initially, a range of Al-containing alloys are being studied before considering coatings with similar Al contents. Both sets of experiments show promising results, consistent with the thermodynamic assessment [8].

2. Experimental procedure

Capsule tests with static Pb–Li (detailed elsewhere [11]) were performed on dense, monolithic, high-purity (99.9995%) chemical vapor deposited (CVD) β-SiC specimens (3 × 8 × 12 mm) fabricated by Rohm and Haas, with a density of 3.21 g/cm^3. To avoid unwanted reactions, the SiC specimen and Pb–Li were contained in CVD SiC capsules and welded Mo intermediate capsules. The 1200 °C experiment used an outer capsule of alloy 602CA (Ni–26 at.%Cr–9Fe–5Al). In all tests, the capsules were loaded with high purity (99.9999%) Pb shot and Li in an argon-filled glove box. Specimen mass was measured before and after exposure on a Mettler–Toledo balance with an accuracy of ±0.04 mg. Exposures were performed in resistively heated box furnaces.

The chemical composition of the Al-containing alloys tested at 700 °C are shown in Table 1. A Fe_3Al composition was selected as being similar to aluminide coatings formed on Fe-base alloys [12,13] and a Ni–42Al composition is similar to the composition of a CVD aluminide coating on a Ni-base alloy [14]. In addition, an oxide dispersion strengthened (ODS) FeCrAl (Plansee alloy PM2000) was tested as this alloy, or similar commercial tubing alloys (e.g. Kanthal alloy APMT), [15] that would not require a corrosion-resistant coating. The 1.5 mm thick specimens had a surface area of 4–5 cm^2 and were polished to a 600grit SiC finish and were not pre-oxidized. They were ultrasonically cleaned in acetone and methanol prior to suspending the specimens in a welded Mo capsule using Mo wire.

After exposure, the specimens were soaked in a mixture of acetic acid, hydrogen peroxide and ethanol for 24–72 h to remove any residual Pb–Li. The composition of the Pb–Li after testing was determined by inductively coupled plasma analysis and combustion analysis. Post-test surfaces were examined using Auger electron spectroscopy (AES), X-ray photoelectron spectroscopy (XPS) and scanning electron microscopy (SEM). Cross-sections of the exposed metal specimens were examined using electron probe microanalysis (EPMA).

3. SiC results

Three capsule experiments where monolithic SiC specimens were exposed have recently been completed: 5000 h at 800 °C, 2000 h at 1100 °C and 1000 h at 1200 °C. A summary of the mass change results for the most recent capsule tests and previous tests [11,16] is shown in Table 2. A statistically significant mass gain was observed after 5000 h at 800 °C while the other tests showed smaller mass gains or losses. Limited reaction at 800 °C is consistent with previous results [17,18]. No change in the specimen surface was visible. However, as with the earlier tests, a small amount of powdery black residue was left on the specimen surface. This was identified as C by AES with trace amounts of Pb and Li detected by XPS.

Table 1
Alloy chemical compositions (at.% or ppma) determined by inductively coupled plasma analysis and combustion analysis

Material	Fe	Ni	Cr	Al	O	C	N	S	Other
316SS	65.1	8.9	19.9	0.02	490	3360	2380	68	1.94Si, 1.67Mn, 1.38Mo, 0.21Cu
ODS FeCrAl	67.8	0.02	20.0	10.6	7430	340	210	50	0.44Ti, 0.23Y, 0.04Si, 0.04Mn
Fe–28Al–2Cr+Zr	70.0	<	2.0	27.9	70	400	<	46	0.026Zr, 0.005Hf
Ni–42.5Al	<	57.3	<	42.6	40	380	<	<	<

< indicates below the detectability limit of <0.01% or <0.001% for interstitials.

Table 2
Mass change of CVD SiC specimens after exposure in Pb–17Li

Material	Temperature (°C)	Time (h)	Mass change	
			(mg)	(mg/cm^2)
SiC	800	1000	−0.02 ± 0.04	−0.01 ± 0.01
		5000	+0.10	+0.03
	1100	1000	−0.02	−0.01
		2000	+0.02	+0.01
	1200	1000	+0.04	+0.01
316SS	700	1000	−17.4	−3.79
ODS FeCrAl		1000	−1.4	−0.20
Fe–28Al–2Cr+Zr		1000	−1.0	−0.25
Ni–42.5Al		1000	−0.4	−0.09

The mass change accuracy for these measurements is shown.

The composition of the Pb–Li after exposure is shown in Table 3. Although previous tests had shown no detectable Si after exposures for 1000 h at 800 °C and 1100 °C, Si was detected after 2000 h at 1100 °C and 1000 h at 1200 °C. (The amount does not necessarily correspond to the specimen mass change because the capsule also was made of CVD SiC.) The presence of Si in the Pb–Li indicates that some dissolution occurred at 1100 °C and 1200 °C and suggests that SiC may be limited to <1100 °C in flowing Pb–Li. These Si levels are still less than the 2100 ppma (350 ppmw) that was reported from EPMA of Pb–Li after exposure of SiC at 800 °C [18]. The O, C and N contents increased after each exposure, however, some contamination could occur during post-test handling. Capsule experiments are being planned with SiC/SiC composite specimens. More interaction may be expected with the SiC fibers or the fiber–matrix interface. However, it is anticipated that a dense CVD-SiC seal coat will cover the outer layer of any SiC composite components [5].

4. Al-containing alloy results

Table 2 shows the mass losses for type 316 stainless steel and the Al-containing alloys exposed for 1000 h at 700 °C in Pb–17Li. Compared to type 316 stainless steel, more than an order of magnitude reduction in the amount of dissolution was observed for the Al-containing alloys based on these mass changes. All of the specimens were characterized after exposure and Figs. 1–3 give examples of those findings. Fig. 1 shows a polished cross-section of the

Table 3
Chemical composition using inductively coupled plasma and combustion analysis of the starting Pb and the Pb–Li after capsule exposures at the indicated temperatures and times (in ppma except for Li in at.%)

Test	Li	Si	C	O	N	Al	Cr	Fe	Mo	Ni	Mn	S
Starting	n.d.	<40	<170	1270	<40	<8	<4	<4	<2	<4	n.d.	n.d.
SiC 1000 h exposure												
800 °C	17.49%	<30	1850	4090	100	6	<3	6	<2	<3	n.d.	n.d.
1100 °C	16.27%	<30	1160	3550	90	<6	<3	6	<2	<3	n.d.	n.d.
1200 °C	15.62%	**370**	2690	16620	450	<20	<10	<10	<5	<10	n.d.	n.d.
SiC 2000 h exposure												
1100 °C	15.99%	**185**	1025	7890	200	<60	<30	<30	<20	<30	n.d.	n.d.
SiC 5000 h exposure												
800 °C	18.55%	<60	650	2580	90	<20	<10	<10	<5	<10	n.d.	n.d.
700 °C, 1000 h exposure												
316SS	17.4%	<60	1590	7440	60	<60	<30	<30	<20	90	<30	900
FeCrAl	17.9%	<60	1260	4140	90	<60	<30	30	<20	<60	<30	370
Fe3Al	16.5%	<60	1520	14860	320	<60	<30	<30	<20	<60	<30	110
NiAl	18.2%	<60	1200	10310	370	<60	<30	840	20	30	<30	1100

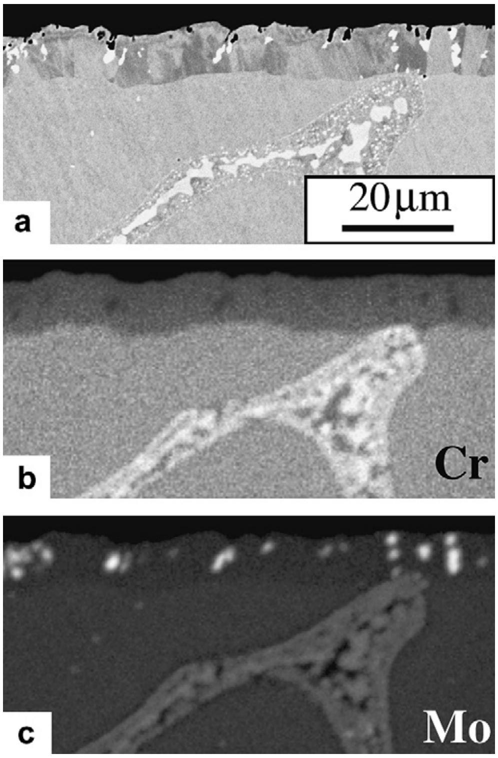

Fig. 1. (a) Secondary electron image of a polished cross-section of type 316 stainless steel after exposure for 1000 h at 700 °C in Pb-17Li. X-rap maps of the same region show the concentration of (b) Cr and (c) Mo. The Cr- and Mo-rich (bright) second phase in the steel is likely sigma or a laves phase.

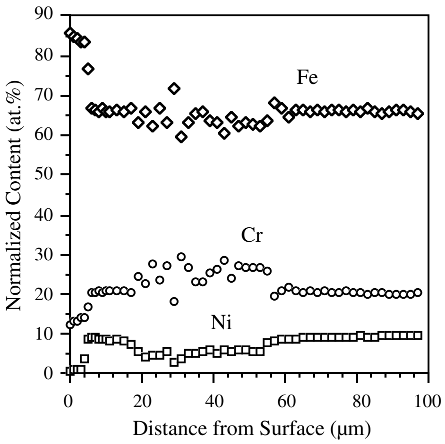

Fig. 2. Composition line profile of a polished cross-section of type 316 stainless steel after exposure for 1000 h at 700 °C in Pb–17Li. The Ni and Cr are depleted from the outer region shown in Fig. 1(a).

type 316 stainless steel specimen after exposure. As expected, there is an outer layer depleted in both

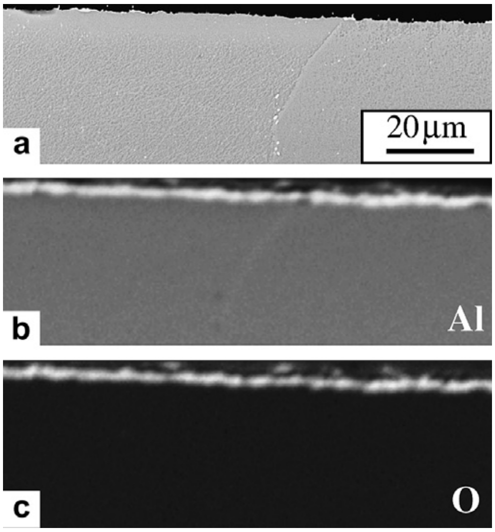

Fig. 3. (a) Secondary electron image of a polished cross-section of Ni–42Al after exposure for 1000 h at 700 °C in Pb–17Li. X-ray maps of the same region show the concentration of (b) Al and (c) O.

Cr (Fig. 1(b)) and Ni (Fig. 2). The mass loss corresponds to a ∼5 µm loss in metal, with Ni and Cr being selectively removed, which is consistent with this observation. The Mo-rich precipitates in the outer layer (bright areas in Fig. 1(c)) are not likely from the Mo capsule, but from the alloy itself, Table 1. Other experiments with 316 specimens and stainless steel or carbon steel capsules for the same time and temperature [16,19] also showed Mo-rich particles in the outer layer consistent with the dissolution resistance of Mo [10].

No depletion layer was observed in the NiAl specimen although selective removal of Ni would be expected. However, a slight depletion in Al was observed near the surface that may be due to Al diffusing outward to form a surface Al_2O_3 layer (the bright layer in Fig. 3(b) and (c)). Similar oxide layers, although less distinct, were observed on the FeCrAl and Fe_3Al specimens. This is a relatively low temperature for the formation of a continuous alumina layer. With the lower Al contents in FeCrAl and Fe_3Al, these specimens may not have been able to form an alumina layer as quickly. The higher mass losses for these materials (Table 2) may be associated with the longer time needed to form a protective alumina layer by gettering O from the Pb–Li.

Table 3 shows the post-test Pb–Li chemistry. Again, the general increase in the interstitial impurities may reflect uptake during handling before and after the test. The high Fe content for the NiAl specimen was unusual as there was no obvious source of Fe. The Ni content was highest for the 316 specimen, 90 ppma. However, this is far below the saturation limit at this temperature. When a 304 stainless steel capsule was used with a 316 specimen, [12] much higher values for Ni (740 ppma), Cr (160) and Mn (380) were detected [19] in the Pb–Li as both the specimen and the capsule walls were dissolving.

Capsule experiments are currently being conducted at 800 °C on pre-oxidized Al-containing alloys and CVD aluminized 316 specimens with and without pre-oxidation. Future work will eventually include flowing liquid metal experiments with a temperature gradient. Static capsule experiments can only be expected to produce a limited compatibility assessment because saturation inhibits further dissolution. Low-cost quartz loops have been used for testing Bi–Li [20]. This concept was assessed by testing Pb–Li in a quartz ampoule at 800 °C for 1000 h. No Si was detected in the Pb–Li after the test.

5. Summary

Static Pb–17Li capsule tests were performed on monolithic SiC specimens and Al-containing alloys. Both systems showed little or no dissolution in Pb–Li, likely due to the formation of a protective surface oxide which was expected to be stable based on thermodynamic evaluations [7,8]. For SiC, Si was detected in the Pb–Li only at the highest test temperatures (2000 h at 1100 °C and 1000 h at 1200 °C). The addition of Al to Fe- or Ni-base alloys resulted in a significant decrease in the amount of dissolution after 1000 h at 700 °C compared to type 316 stainless steel. Bare metal samples formed an Al_2O_3 surface layer, especially for the highest Al content material, Ni–42.5%Al. These results suggest that aluminide coatings could protect a wide range of conventional Fe- or Ni-base tubing alloys to carry Pb–Li between the first wall and the heat exchanger. Future work will need to include testing in a flowing system with a thermal gradient to fully determine the compatibility of these materials.

Acknowledgments

The research was sponsored by the US Department of Energy (DOE), Office of Fusion Energy Sciences, Fusion Energy Materials Program, under contract DE-AC05-00OR22725 with UT-Battelle, LLC. D.F. Wilson and J.R. DiStefano consulted on the experimental procedure. H. Longmire and L. Walker assisted with the experimental work. S.J. Pawel, J.R. DiStefano and S.J. Zinkle provided comments on the manuscript.

References

[1] P. Noajitra, L. Bühler, U. Fischer, S. Malang, G. Reimann, H. Schnauder, Fusion Eng. Des. 61&62 (2002) 449.
[2] M. Abdou, D. Sze, C. Wong, M. Sawan, A. Ying, N.B. Morley, S. Malang, Fusion Sci. Technol. 47 (2005) 475.
[3] G. Benamati, C. Fazio, I. Ricapito, J. Nucl. Mater. 307–311 (2002) 1391.
[4] J. Konys, W. Krauss, Z. Voss, O. Wedemeyer, J. Nucl. Mater. 329–333 (2004) 1379.
[5] B. Riccardi, L. Giancarli, A. Hasegawa, Y. Katoh, A. Kohyama, R.H. Jones, L.L. Snead, J. Nucl. Mater. 329–333 (2004) 56.
[6] T. Yoneoka, S. Tanaka, T. Terai, Mater. Trans. 42 (2001) 1019.
[7] P. Hubberstey, J. Nucl. Mater. 247 (1997) 208.
[8] P. Hubberstey, T. Sample, A. Terlain, Fusion Technol. 28 (1995) 1194.
[9] T. Flament, P. Tortorelli, V. Coen, H.U. Borgstedt, J. Nucl. Mater. 191–194 (1992) 132.
[10] H. Feuerstein, H. Gräbner, J. Oschinski, S. Horn, J. Nucl. Mater. 233–237 (1996) 1383.
[11] B.A. Pint, L.D. Chitwood, J.R. DiStefano, Fusion Materials Semi-Annual Reports, DOE-ER-0313/35, Oak Ridge, TN, (2003) 13.
[12] N.V. Bangaru, R.C. Krutenat, J. Vac. Sci. Technol. B 2 (1984) 806.
[13] Y. Zhang, B.A. Pint, G.W. Garner, K.M. Cooley, J.A. Haynes, Surf. Coat. Technol. 188&189 (2004) 35.
[14] Y. Zhang, W.Y. Lee, J.A. Haynes, I.G. Wright, B.A. Pint, K.M. Cooley, P.K. Liaw, Metall. Trans. 30A (1999) 2679.
[15] B. Jönsson, R. Berglund, J. Magnusson, P. Henning, M. Hättestrand, Mater. Sci. Forum 461–464 (2004) 455.
[16] B.A. Pint, J.L. Moser, P.F. Tortorelli, Fusion Eng. Des. 81 (2006) 901.
[17] F. Barbier, Ph. Deloffre, A. Terlain, J. Nucl. Mater. 307–311 (2002) 1351.
[18] H. Kleykamp, J. Nucl. Mater. 321 (2003) 170.
[19] B.A. Pint, P.F. Tortorelli and J.L. Moser, Fusion Materials Semi-Annual Reports, DOE-ER-0313/38, Oak Ridge, TN, (2005) 89.
[20] J.R. DiStefano and O.B. Cavin, Report # ORNL/TM-5503, 1976, Oak Ridge National Laboratory, Oak Ridge, TN.